

Interstitial mechanisms for plastic flow in the initial stage of loading during microindentations

Yu. I. Golovin and A. I. Tyurin

Tambov State Pedagogical Institute, 392000 Tambov, Russia

(Submitted 16 August 1994; resubmitted 20 October 1994)

Pis'ma Zh. Eksp. Teor. Fiz. **60**, No. 10, 722–726 (25 November 1994)

Quantitative data are found on the dynamics and microscopic mechanisms of the initial stage (0–10 ms) of the loading of the hard indenter in ionic crystals with the NaCl lattice. In particular, values have been found for the contact stress and the activation volume. The typical values of this volume are a few tenths of the volume occupied by an ion in the lattice. This result, combined with the high contact stress (up to a third of the Young's modulus), points to a predominantly interstitial mechanism for mass transport in the early stages of the loading of the indenter. © 1994 American Institute of Physics.

Back in the early 1970s, an interstitial mass transport for plastic flow,^{3–6} which was well known in radiation physics, was proposed along with the microscopic mechanisms based on dislocations^{1,2} and vacancies. Indirect evidence for a possible nondislocation plasticity in the formation of the imprint as a hard indenter penetrates into the surface of a crystal has been found by electron microscopy, microcathodoluminescence, and other methods.^{3,4,7} However, there are as yet no direct, convincing quantitative data demonstrating the reality of interstitial mass transport. It follows from the general considerations discussed in Refs. 3, 5, and 6 that the probability for observing this transport increases with increasing stress (or pressure) and with decreasing temperature. The situation in which the necessary conditions can be arranged most easily is under the indenter in the initial stage of the indentation. However, the overwhelming majority of the results on the processes accompanying indentation have been found through studies of the size and shape of the imprint and the morphology and structure of the surrounding zone which have been carried out *after* the indentation. There have been a few studies of the kinetics of the final, slow stage of the indentation,^{1,8,9} but essentially no information is available on the fast initial stage (≤ 0.1 s), during which up to 80–90% of the volume of the material is displaced from beneath the indenter. As a result, we do not know the contact stress which actually arises, nor do we know the penetration rate or other quantitative facts which would make it possible to draw conclusions about the microscopic mechanisms for the displacement of the material from beneath the indenter. The most informative results available are on activation parameters, especially the activation volume, which characterizes the dimensions of the region in which the elementary mass-transport event occurs.

In this paper we are reporting preliminary data on the dynamics and thermal-activation parameters of the process by which the indenter enters the material in the first 10–20 ms after the motion begins. The apparatus and procedure of Ref. 10 made it possible to continuously measure the indenter displacement $h(t)$ as it enters the material,

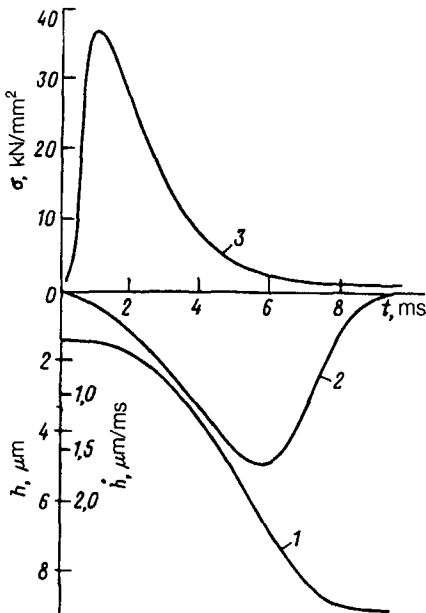


FIG. 1. Kinetics of the initial stage of the penetration of the indenter into a LiF (001) face at room temperature. 1— $h(t)$; 2— $\dot{h}(t)$; 3— $\sigma(t)$.

without an initial velocity, with a time resolution better than 1 ms. Knowing the actual kinetics of the penetration, we can determine the instantaneous value of the contact stress $\sigma(t)$ under the indenter, working from the obvious equation

$$m\ddot{h}(t) = mg - k\sigma(t)h^2(t),$$

where m is the mass of the moving tip with the indenter, \ddot{h} is the acceleration of the indenter, which is found by double differentiation of the function $h(t)$, and the coefficient $k = 26.5$ reflects the particular geometry of the indenter.

Experiments were carried out on the ionic crystals NaCl, KCl, LiF, and MgO with various impurity contents over the temperature range $T = 77\text{--}300$ K. The results turned out to be qualitatively the same. It follows from the typical dynamic curves (Fig. 1) that the first stage of the increase in $h(t)$ corresponds to motion of the indenter with a positive acceleration, while the second, which begins at 6–8 ms (for the various crystals), corresponds to motion with a negative acceleration, but the acceleration never exceeds 0.5 m/s^2 in absolute value. Such low values of the acceleration are evidence that, even after the first few milliseconds of the motion, with $h \sim 1$ μm , the material of the sample develops a resistance to the motion of the indenter—a resistance which is nearly equal to the weight of the moving parts of the loading apparatus. It can be seen in Fig. 1 that $\sigma(t)$ initially reaches values of 35 ± 10 kN/mm^2 (about a third of the Young's modulus). Over the next 8–9 ms, $\sigma(t)$ falls off to ~ 1 kN/mm^2 , close to the steady-state microhardness of LiF. Up to 6 ms, the indentation rate typically rises monotonically, despite the rapidly decreasing stress at the contact. This behavior of the material might be explained on the basis that the viscosity decreases as time elapses (the decrease would amount to about an order of magnitude over the first 5 ms). However, it is extremely difficult to name any specific mechanism for this thixotropy. The simplest assumption—that we are

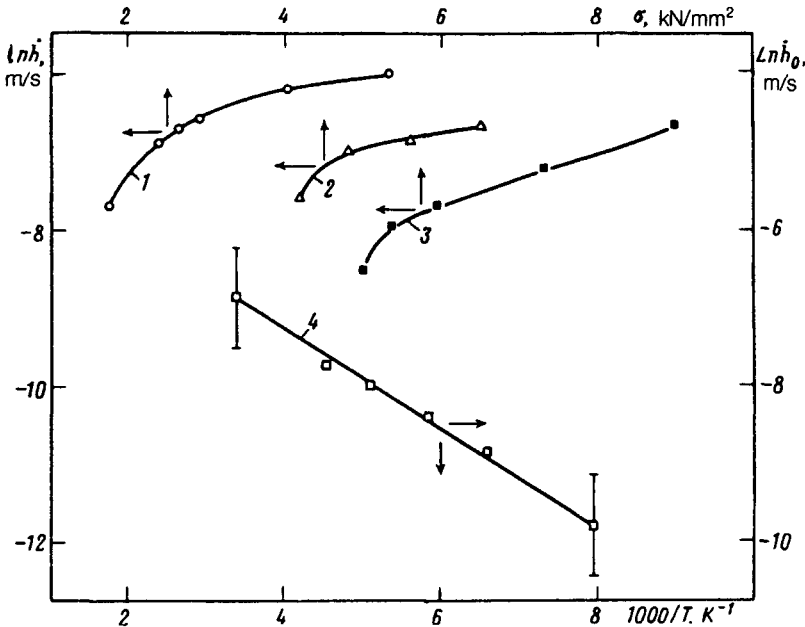


FIG. 2. Plot of $\ln \dot{h}$ versus σ and of $\ln \dot{h}_0$ versus $1/T$ for LiF crystals. 1–3) $\ln \dot{h}(\sigma)$ at $T = 293, 196,$ and 126 K, respectively; 4) $\ln \dot{h}_0(1/T)$.

seeing an effect of heating during flow—breaks down under order-of-magnitude checks of the value of ΔT (an upper estimate is $\Delta T \leq 0.1$ K). The ultrahigh stress which arises under the indenter in this stage probably renders the material amorphous, with the result that the material acquires properties of a thixotropic medium. Such a situation is typical of high-viscosity liquids and polymers, not of crystalline solids.

Indications of a change to an amorphous structure have been seen by other investigators, working by independent methods. Page *et al.*,¹¹ for example, observed an abrupt expulsion of an indenter when the load reached a certain critical level in nanoindentation of silicon (i.e., during puncture at very low loads, $\sim 10 \mu\text{N}$, which created imprints ~ 100 nm across). Using electron microscopy, they observed a severely damaged region under the indenter after complete loading. They believe¹¹ that these results indicate a phase transition induced by the high hydrostatic pressure, which reached some tenths of the Young's modulus, as in our own experiments.

The second stage of the penetration of the indenter, in which \dot{h} decreases with increasing σ , can be analyzed by conventional approaches. A plot of the force dependence of the loading rate in the coordinates $\ln \dot{h} = f(\sigma)$ has regions which are approximately linear (Fig. 2). We can thus extrapolate to $\sigma = 0$ to find the initial penetration rate \dot{h}_0 at various temperatures T . The plot of $\ln \dot{h}_0 = f(T^{-1})$ also turns out to be approximately linear (Fig. 2), indicating that the penetration processes are thermally activated in the range $T = 125\text{--}300$ K. In the second stage of the penetration ($5 \leq t \leq 8$ ms), the

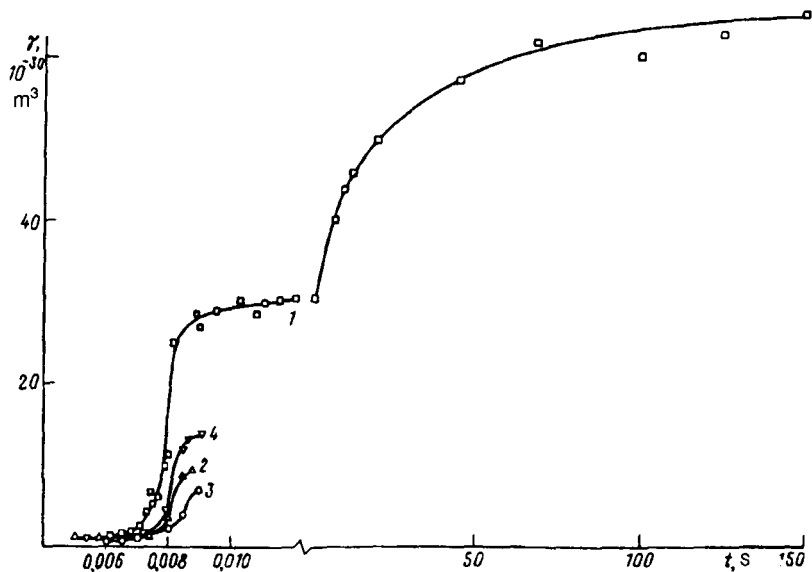


FIG. 3. Activation volume versus the indentation time for several ionic crystals at room temperature. 1—LiF; 2—NaCl; 3—KCl:Ba; 4—MgO.

activation volume γ found from the slope of $\ln \dot{h}(\sigma)$ has very low values, $\gamma \approx 10^{-30} \text{ m}^{-3}$, for all the crystals studied (Fig. 3). The corresponding activation energies U^* are about 0.1 eV. Such low values of U^* and γ are evidently due to the high values of σ in this stage, in which only elastic strain can reach a value of a large fraction.

The activation volumes, which amount to a few tenths of the volume (V_0) occupied by a cation in the lattice, are direct evidence of a deformation due to motion of individual atoms.^{5,6} Experiments on the effect of hydrostatic pressure on the diffusion rate yield similar values,¹² $V = (0.6-0.7)V_0$. In the absence of reliable independent data on the activation parameters for the nucleation and motion of interstitial atoms and vacancies at high pressures ($\sim 0.1-1$ Mbar), we have no rational basis for deciding between these two possibilities, although interstitial (crowdion) mechanisms naturally become more likely with increasing compressional stress. In the later stages, when σ begins to approach the static microhardness ($t \geq 10$ ms), U^* increases to 0.2–0.3 eV, and γ to $\sim 10^{-28} \text{ m}^3$, i.e. $\sim 10b^3$, where b is the Burgers vector of gliding dislocations. This result agrees with the data of Refs. 1 and 9 and indicates that a dislocation flow mechanism is predominant.

Admittedly, the error in the determination of the quantities U^* and γ by the method described above is large ($\sim 30-40\%$), and we have furthermore ignored the nonuniformity of the applied stress and the existence of internal stress. Still, incorporating these and other factors could not change U^* or γ in order of magnitude and thus could not cast doubt on the basic conclusion of this study: that point defects play an important role in the mass transport in the initial stage of indentation, even in such soft crystals as NaCl and KCl. For harder materials we would expect an even greater role from nondislocation

mechanisms for the expulsion of material from beneath the indenter.

We wish to thank V. I. Al'shits, A. A. Urusovkaya, and M. I. Akchurin for useful discussions of these results and for valuable comments.

- ¹ Yu. S. Boyarskaya *et al.*, *Physics of Microindentation Processes* [in Russian] (Shtiintsa, Kishinev, 1986).
- ² Yu. S. Boyarskaya *et al.*, *Izv. Akad. Nauk SSSR, Neorg. Mater.* **26**, 1017 (1990).
- ³ V. N. Rozhanskiĭ *et al.*, *Phys. Status Solidi* **41**, 579 (1970).
- ⁴ V. N. Rozhanskiĭ *et al.*, *Fiz. Tverd. Tela (Leningrad)* **13**, 411 (1971) [*Sov. Phys. Solid State* **13**, 335 (1971)].
- ⁵ V. L. Indenbom, *JETP Lett.* **12**, 526 (1970).
- ⁶ V. L. Indenbom and A. N. Orlov, *Fiz. Met. Metalloved.* **43**, 469 (1977).
- ⁷ M. Sh. Akchurin *et al.*, *Fiz. Tverd. Tela (Leningrad)* **30**, 760 (1988) [*Sov. Phys. Solid State* **30**, 435 (1988)].
- ⁸ M. S. Kats *et al.*, *Fiz. Tverd. Tela (Leningrad)* **17**, 922 (1975) [*Sov. Phys. Solid State* **17**, 1945 (1975)].
- ⁹ S. I. Bulychev *et al.*, *Fiz. Khim. Obr. Mater.*, No. 5, 69 (1979).
- ¹⁰ Yu. S. Boyarskaya *et al.* *Latv. Fiz.-Tekhn. Zh.*, No. 4, 65 (1991).
- ¹¹ T. F. Page *et al.*, *J. Mater. Res.* **7**, 450 (1992).
- ¹² V. I. Zaitsev *et al.*, *Fiz. Tverd. Tela (Leningrad)* **17**, 1866 (1975) [*Sov. Phys. Solid State* **17**, 1227 (1975)].

Translated by D. Parsons